Science of the Total Environment 924 (2024) 171518

Contents lists available at ScienceDirect

Science of the Total Environment

journal homepage: www.elsevier.com/locate/scitotenv

Enhancing nutrient absorption through the influence of mangrove ecosystem on flow rate and retention time in salt marshes

Sadegh Partani [a], Ali Danandeh Mehr [b,c,*], Ali Jafari [a,d]

[a] Department of Civil Engineering, Faculty of Engineering, University of Bojnord, Bojnord, Iran
[b] Civil Engineering Department, Antalya Bilim University, Antalya, Turkey
[c] MEU Research Unit, Middle East University, Amman, Jordan
[d] Modares Environmental Research Institute, Tarbiat Modares University, Tehran, Iran

HIGHLIGHTS

- The impact of pneumatophores on flow rate, retention time, and contact time was investigated.
- The impact of pneumatophores on nutrient absorption through the sediment was investigated.
- By increasing the density of mangroves in salt marshes the absorption rate was increased.
- Pneumatophores serves as an effective sink for organic matters in Chabahar Bay.

GRAPHICAL ABSTRACT

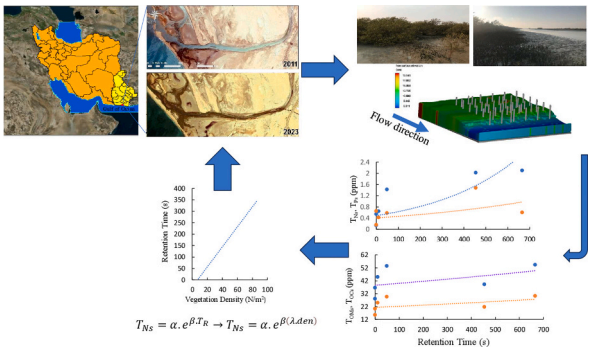

ARTICLE INFO

Editor: Paromita Chakraborty

Keywords:
Contact time
Coastal wetland
Mangrove ecosystem
Pneumatophores
Velocity
Retention time
Plant density
Nutrients

ABSTRACT

This study investigates the impact of pneumatophores (the aerial roots of Avicenna marina) on water flow rate, retention time, contact time, and consequently on nutrient absorption through the sediment in sub-tropical salt marshes. The goal is to realize how the density of mangroves in salt marshes influences the kinematic factors of streamflow at estuaries. To this end, a field experiment was carried out to assess nutrient and organic compound levels in the sediment and water samples, spanning six sampling stations along the Chabahar River discharging to the Chabahar Bay, Iran. Then, we delved into the influence of altering environmental parameters, such as density and geometry, on the kinematic features of the flow through statistical analysis and hydraulic modeling. The results showed that the aerial roots reduce the flow rate and increase both retention and contact times. The longest retention time was observed at station #5 due to increased vegetation density and decreased instream velocity. In addition, measurements of total organic matter, total organic carbon, and total nitrogen indicated that an extended contact time resulted in increased absorption flux to the stream by sediments. As a result, pneumatophores can serve as an effective sink for organic matter in ecotones in salt marshes.

* Corresponding author at: Civil Engineering Department, Faculty of Engineering and Natural Sciences, Antalya Bilim University, 07190 Döşemealtı, Antalya, Türkiye.
E-mail address: ali.danandeh@antalya.edu.tr (A. Danandeh Mehr).

https://doi.org/10.1016/j.scitotenv.2024.171518
Received 13 January 2024; Received in revised form 4 March 2024; Accepted 4 March 2024
Available online 8 March 2024

1. Introduction

Over the last few decades, the rise in urbanization, industrial, and agricultural activities has led to a significant increase in the number of vegetation islands. The existence of vegetation islands profoundly influences sediment and nutrient transport, shaping the overall hydraulic dynamics of water bodies (Li et al., 2023a; Zhu et al., 2023). The growth of vegetation can create resistance against the flow having temporary or long-term effects on sedimentation patterns. The coastal vegetation in a river system can cause a decrease in flow velocity, which in turn increases the retention time and roughness of the riverbed (Nardin et al., 2016). This may enhance the shearing stress of the vegetation and its ability to directly absorb sediment, particularly in the canopy of vegetation, and improve sediment retention in salt and freshwater marshes (Nardin et al., 2016; Sadio and Faye, 2023; Van Dijk et al., 2013). The trapping effect occurs when sediment is transported to islands and the vegetation present enhances its persistence (Olliver et al., 2020). This effect is achieved through the absorption of organic matter into the roots of plants (Li et al., 2023b; Zhao et al., 2022). In general, vegetation development in a stream corridor interrupts the normal functioning of streams, reduces flow velocity, and increases shearing stress, resulting in increased flooding risk (van Hespen et al., 2023; Liu et al., 2008). Many research studies have examined how vegetation resistance impacts the flow of rivers, and numerous simulations have been conducted to better understand the connections among flow, vegetation density, nutrient absorption, and sediment transport (Zhang et al., 2023; Liu et al., 2023; Carollo et al., 2005).

Mangroves (pneumatophores) are a type of coastal wetland ecosystem that thrives in tropical and subtropical regions, specifically in intertidal areas and saltwater (Hamilton and Casey, 2016). Recent studies have shown that high productivity of mangroves is achieved where nutrients limit growth through efficient nutrient cycling (Reef et al., 2010). Certain alterations in land use, such as increased sediment and nutrient inputs, are likely to have positive impacts on mangrove nutrient cycles. Conversely, changes associated with eutrophication may lead to adverse consequences (Alongi, 2018). The existence of mangroves at the boundary between land and sea has an influence on flow and plant hydraulics influencing not only water flux and carbon gain but also nutrient uptake and biomass allocation (Yoshikai et al., 2022; Lovelock et al., 2004). The study on the effect of nutrient enhancement on growth, photosynthesis, and hydraulic conductance of dwarf mangroves showed that the introduction of nitrogen and phosphorus induces significant alterations in both tree growth and the internal nutrient dynamics of mangroves in Bocas del Toro, Panama (Lovelock et al., 2004). Empirical evidence underscores the substantial influence of plant-soil feedback on ecological processes (Wen et al., 2024).

Mangroves can alleviate flow velocity and cause sediment deposition and retention. This is due to the presence of aboveground root systems that create drag against the flow of water (Wimmler et al., 2021). Rich biotic interaction in mangrove ecosystems made these areas a source of nutrients for aquaculture (Akram et al., 2023) and sink for deposition of suspended solid load in estuaries that may cause the erosion control associated with salt marshes vegetation (Yasmeen et al., 2024). Mangroves can also retain carbon in their soil systems for a prolonged period due to the presence of anaerobic conditions and high sedimentation rates (Kandasamy et al., 2021). Sediments trap and store enormous amounts of total organic carbon (T_{OC}) and total organic matter (T_{OM}) in very productive coastal wetlands such as mangroves, salt marshes, and seagrass beds (Nellemann and Corcoran, 2009). Thus, clarifying carbon sources plays a key role in understanding the productivity of coastal ecosystems, as well as the transport and transformation of organic matter (Yang et al., 2013). In salt marshes, the sources of organic carbon are marine vegetation habitats, especially mangroves (Kang et al., 2017). The organic carbon content increases by increasing mangroves and the reproduction of new species due to anthropogenic activities (Naidu et al., 2022). The worldwide concern regarding the contamination of mangrove ecosystems with toxic elements, extra loads of nutrients, and heavy metals via the wash/sediment load is increasing. A recent study conducted by Ahmed et al. (2022) demonstrated that salinity reduces site quality and mangrove forest functions.

Our review showed that the earlier studies have mostly investigated the nutrient dynamics of mangroves and their productivity. The studies also indicated that mangroves have an ecological resiliency facing physical water quality and climate change (Nie et al., 2023; Pawar, 2013; Baubekova et al., 2024). However, a limited number of studies have investigated both hydrodynamics and water quality in Mangrove wetlands (Struve and Falconer, 2001; Lam et al., 2023). Differing from earlier studies, our study explores the effect of pneumatophores (aerial roots of Avicenna marina) on both nutrient absorption and flow hydraulics (focusing on flow rate, retention time, and contact time) in salt marshes. We aimed to find the role of mangroves on streamflow and contact time and consequently on chemical water quality exchange between water and sediment in mangroves' wetlands as an ecotone interface of terrestrial and aquatic ecosystems. Given the importance of synchronized assessment of marine contamination and terrestrial pollution transferred by rivers, our study was accomplished along the Chabahar River releasing to the Chabahar Bay, Iran. The study area is about to be classified as a national marine park and a biosphere reserve that hosts some red-list species of the International Union for Conservation of Nature (IUCN). So, the habitat has substantial importance from different points of view. The findings are anticipated to offer valuable insights for researchers engaged in comparative studies, serving as a resource for nature conservation organizations and strategies. These insights can contribute to the development of effective nature-based protection methods, particularly for rural communities, which play a pivotal role as main stakeholders in the human ecology cycle. To the best of the authors knowledge, no study has explored the flow rates, retention time, and contact time caused by Pneumatophores density in natural streams so far. Moreover, in this research, the adsorption potential of coastal plants and its effects on water and sediment quality have also been investigated.

2. Material and methods

2.1. Study area

One of the important environmental features of the shallow coastline in the northern region of the Persian Gulf and Sea of Oman is the extended Mangrove Forest with rich biodiversity and an important ecosystem (Rostami et al., 2022; Zahed et al., 2010). Our study area is located at 25°.24' North latitude and 60°.36' East longitude, in the southeast of Iran at Makran coastline and the northern region of the Sea of Oman (Fig. 1). The mean annual rainfall in this area is equal to 117 mm with high inter-annual variability due to the influence of the Indian subcontinent monsoon. Air temperature varies in the range of 18 °C to 32 °C with an average annual of 25.8 °C (Zahed et al., 2010). The area is affected by the sea tide which is about 350 ha in some areas with dense vegetation and others with little or no vegetation. The length of the study path is 4700 m from the beginning of vegetation to the entrance to Chabahar Bay, which is connected to the wetland by a canal at about 200 m after the vegetation starts.

The study area is near the free-trade zone and is poised to evolve into one of the international industrial zones. The development of international tourism infrastructures upstream of the Chabahar rivers is accompanied by urban pollution that has the potential to accumulate in Chabahar Bay. Consequently, the study area serves as a prototype for comparable habitats in sub-tropical zones.

The Hara forests, a distinctive ecosystem in the eastern part of Chabahar, harbor a unique mangrove tree species identified as *Avicennia marina*. Within Iran and specifically in this region, the predominant mangrove species are *Avicennia marina* and *Avicennia germinans* (Partani et al., 2023; Behrooz et al., 2024; Numbere, 2018), representing two of

the three most frequently found mangrove species in sub-tropical coastal zones worldwide. These species, which can grow between three to eight meters tall, are characterized by their aerial roots that become visible during the ebb and flow of the tides. Covering an area of approximately 350 ha, the Hara forests are situated just 1.2 km away from the Free Chabahar Industrial Zone. The region is also experiencing an expansion in petrochemical industries, along with the establishment of a steel factory.

The Chabahar Bay water flows into the river during high tide and sinks during low tide. The study route, extending from the plant growth site to the sea, spans 4700 m. Since 2011, a noticeable increase in vegetation density has been observed in the study area (Fig. 2) (Karsch et al., 2023). This highlights the dynamic nature and continuous evolution of this ecosystem, which is the first hypothesis of this study.

2.2. Sampling stations and field measurements

In this study, water sampling was carried out at six stations along the study area (see Fig. 1 and Table 1) according to the international standards listed in Table 2. The samples were collected using a polyethylene (plastic) bottle, and promptly stored in a cool box at a temperature 4 °C using dry ice. This storage method ensured the protection of the water samples during transportation to the laboratory, where the levels of heavy metals and nutrients were analyzed. Subsequently, the flow velocities were measured at the stations utilizing a cork and a stopwatch. In addition, bathymetry was conducted through traditional field surveys using a plumb line and scale to determine cross sectional geometry and water surface elevation at each sampling station. It is important to note that these measurements were carried out prior to the lowest tide height when the water level was high enough to flow through the roots.

Using the field measurements and lab analysis, the hydraulic simulation and statistical analysis were conducted to figure out how the plant density affects T_{OM} in sediment (T_{OMs}), total nitrogen in sediment (T_{Ns}), T_{OC} in sediment (T_{OCs}), and total phosphorous in sediment (T_{Ps}) along the river.

2.3. Retention time and contact time

Wetlands retention time is usually described as the travel time from inlet to outlet of the desired control volume. The wetlands retention time is sometimes used interchangeably with hydraulic retention time in constructed wetlands. To avoid confusion with the hydraulic retention time in wastewater treatment process and hydrologic concept for routing storm water through detention basins, the term retention time (T_R) is preferred in this study. As expressed in Eq. (1), T_R is defined as the ratio of the volume of the control volume $\forall$ (between two chain-sections) to the discharge, Q, of water passing the volume. In fact, T_R approximates the time required for one complete volume exchange in the wetland.

$$T_R = \frac{\forall}{Q} \tag{1}$$

The contact time (T_{Sc}) is the ratio of distance, L (between two chain-sections), over the velocity between the roots.

$$T_{Sc} = \frac{L}{V_{pa}} \tag{2}$$

3. Results and discussion

Based on observations and measurements made at six designated

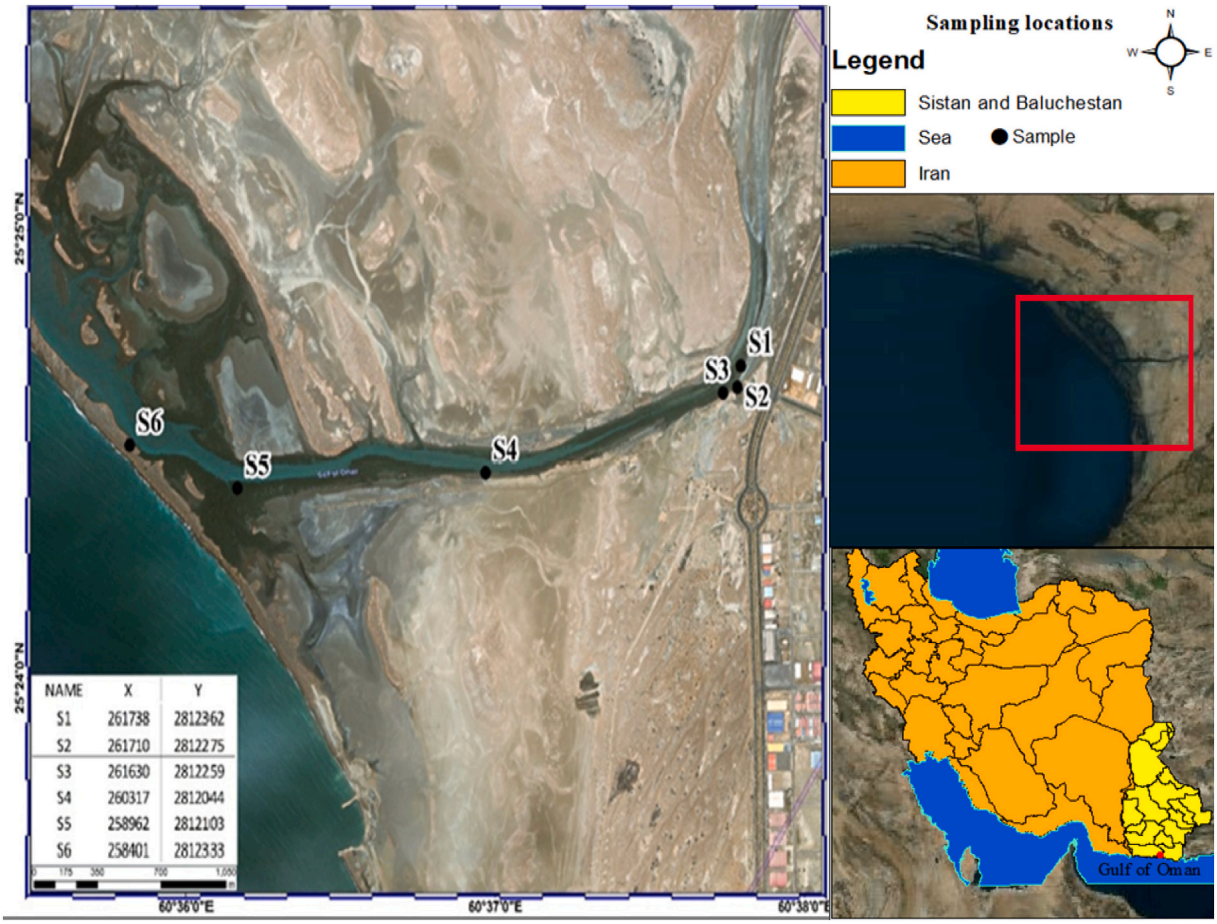

Fig. 1. Map of the study area (Chabahar Bay) and the sampling stations.

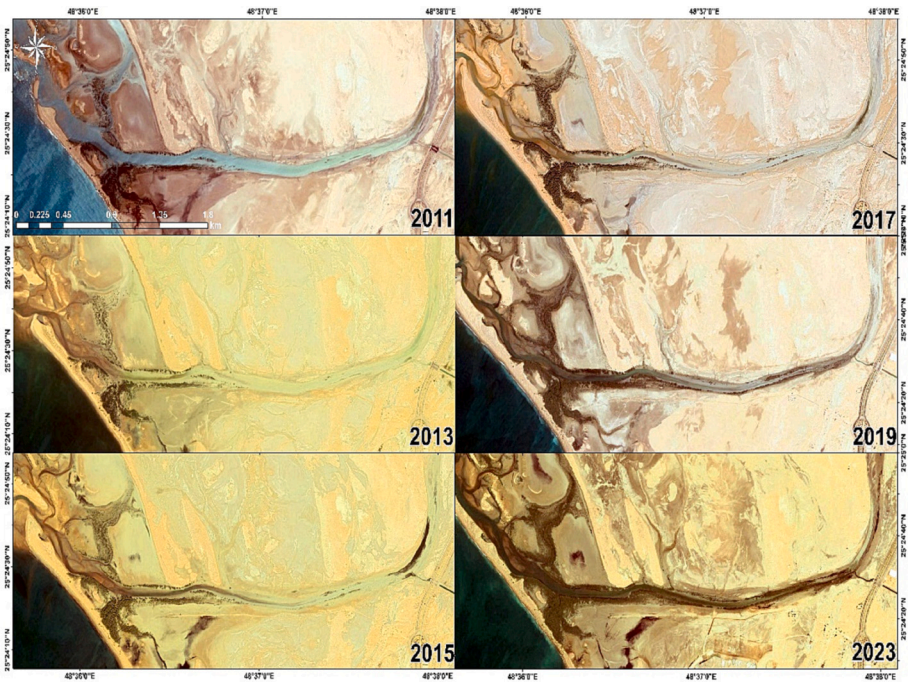

Fig. 2. Vegetation changes in the period 2011–2023.

Table 1
Location of sampling stations and their distance from the entrance to Chabahar Bay.

Station	Location	Distance (m)
S1	100 m before connecting sewer canal	100
S2	Sewer canal	
S3	100 m after connecting the sewage canal to the industrial city	300
S4	Beginning of the connected and massive cover	1650
S5	1.5 km before the end of the wetland terminal	2845
S6	1200 m before connecting to sea / end of vegetation	3500

Table 2
Sampling standards used in this study.

#	Title
1	Water Quality Surveys WHO / UNESCO (Water IWWG on Q of, 1978)
2	USEPA- Method 1669- Sampling Ambient Water for Trace Metals (EPA US, 1996)
3	USEPA, SESDPROC-200-R3, Sediment Sampling (Simmons, 2014)
4	Plant Sampling Guidelines (Johnson and Morgan, 2010)

stations (see Table 2), there is negligible water at station 1 during low tide. Water enters the wetland path from the drainage channel (Station 2) and flows into the sea. Due to the frequent occurrence of tides over time, water washes away surface sediments at Station 3, creating a deep path on the right side of the stream with a small width that increases flow velocity. For this reason, Ebrahimi et al. (2016) studied the effects of plant cover on flow hydraulics and bed form and demonstrated that the passage of flow causes washing of sediment from areas that lack vegetation cover, which has been a small vortex flow with high velocity from a hydraulic point of view. The water flows to Station 4 (towards the coast) along the waterway, then due to sedimentation and reduced flow velocity, the depth of the flow path decreases. At the interface of terrestrial area and aquatic ecosystem, soluble materials and suspended sediments create a suitable bed for sedimentation and plant growth. The reasons behind are the local topographic features as well as the diminishing water depth/velocity due to dense forest at Station 5. As discussed in (Mahsa and Afzalimehr, 2017), vegetation cover increases tensile force and deflects flow, leading to a decrease in horizontal velocity. The variables that used to measure water flow rate in the desired sections of the river are measured and calculated in Table 3; where Q_{pa} is the flow rate between roots, Q_{avg} is the average flow rate, A_{pa} is the measured area of roots, A is the cross-section area of sampling stations, V_{pa} is the flow velocity between roots, V_{max} is the highest velocity at each cross section, and V_{mean} is the average velocity at each section.

Fig. 3 shows how V_{pa} and V_{mean} vary along the river. As shown in the figure, the average velocity is affected by the tidal phenomenon in stations 2 and 3. The velocity at the third station reaches its maximum level, and after 1.4 km, the average velocity starts to decrease. Station 5 has the minimum measured velocity and has the most vegetation cover and cross-sectional area of the station, then at the sixth station, the water velocity starts to increase.

Table 4 tabulated the results of field measurements and hydraulic features calculated at each station. Here, L_s denotes the length of the vegetation path. As shown in the table, flow velocity and discharge are seen at station 2 between the roots due to the absence of plants along the coast.

The marsh's initial flow commenced from the second station, given the marshy conditions at the first station, and proceeded through subsequent stations until reaching the sea. Upon entering the main channel at the intersection, the flow resulted in the erosion of bed materials. The emptying and filling of the marsh every day due to tides is also a factor in sediment transport towards the sea, increasing erosion (Ebrahimi et al., 2016). The wastewater flow from the drainage channel (second station) is connected to the main channel at the lower point of the first station and the upper point of the third station. At the point of flow connection, the soil bed is washed away, and the waterway path creates a narrower width but with a steeper slope and greater depth, which increases the water velocity. While the water begins to discharge, water seeps between the roots, except for direct movement towards the center of the flow path, due to the difference in elevation between the sides of the waterway. After covering 1100 m, the vegetation decreases, and after 200 m, it starts to grow again. After 100 m, we reach the fourth station, has more vegetation cover than the third station. The water flow from

Table 3
Measurement results of velocity components at stations.

Station	Q_{pa}/Q_{mean}	A_{pa}/A	V_{pa}/V_{max}	Q_{pa} (m^3/s)	V_{pa} (m/s)	A_{pa} (m^2)	Q_{avg} (m^3/s)	V_{mean} (m/s)	V_{max} (m/s)	A (m^2)	Density (No./m^2)
S1	0 %	0 %	0 %	0	0	0	0.02	0.09	0.14	0.25	39
S2	0 %	0 %	0 %	0	0	0	0.52	0.1	0.12	5.23	0
S3	10 %	25 %	27 %	0.07	0.08	0.88	0.66	0.19	0.28	3.53	56
S4	9 %	12 %	70 %	0.09	0.06	1.51	1	0.08	0.09	12.9	84
S5	2 %	4 %	39 %	0.02	0.02	1.2	1.39	0.04	0.05	31.77	86
S6	1 %	2 %	49 %	0.018	0.04	0.45	1.62	0.07	0.09	24.89	48

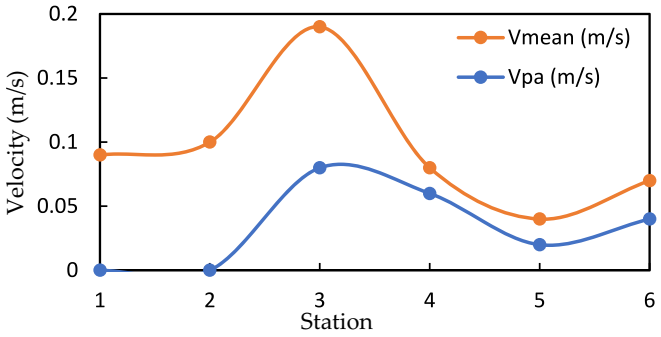

Fig. 3. Ratio of average velocity to velocity between roots at stations.

the third station, moving downstream, due to topographic conditions and the increase in width of the waterway and vegetation cover and depth, causes a decrease in flow velocity and an increase in discharge. The retention time at this station increases due to these reasons. Moving one kilometer downstream from the third station, there is a noticeable increase in vegetation cover. The sampling time, influenced by the declining water level during tides, leads to a reduction in depth and a finer grain size compared to the other stations, attributed to the lower flow velocity. In this station, the cross-sectional width and flow velocity decrease on the sides and the main channel, which leads to an increase in retention time.

3.1. The effect of roots and their density on water flow

As already mentioned, mangrove is the dominant vegetation cover in the study, which has cone-shaped pneumatophores aerial roots (Fig. 4). Typically, the height of the roots reaches 30 cm, and the diameter of the roots reaches 3 cm. Vegetation modeling has been done with Flow3D software. Vegetation density for two stations was modeled. The modeling in the software was considered based on centimeter-gram-second system and the type of turbulent incompressible flow, and the roughness coefficient was considered 0.095. The flow was chosen to be viscous. The renormalization group model was used to solve turbulence. The distribution of hydrostatic flow pressure in the Z direction has been considered. Initially, as the water flow encounters mangrove, the water depth increases. After stabilizing the water flow in the roots, the depth begins to decrease. The water level reaches up to 12 cm in the initial range, and in this way, the effect of the roots on the flow depth becomes evident.

The data collected from various sections revealed that the first station lacks a permanent flow, with water reaching this section only at the sea's highest level during tides. As the ebb tide begins, water rapidly drains from this marsh segment, leading to sediment formation in the channels between the roots. Root density at this station was measured to be 39 roots per square meter (Table 3). The second station, a sewage channel, experiences weak flow compared to the tides. The water in the channel is tide-dependent, and during ebb tides, it flows shoreward from the channel. Given the absence of vegetation cover at the second station, density measurement was disregarded. The third station, situated 100 m beyond the permanent flow's start, corresponds to the industrial park's (S1) sewage channel. Along this path, vegetation cover intensifies with the density measured as 56 roots per square meter. After traveling 1500 m, the vegetation cover diminishes, only to reappear at 1600 m with increased density. At the fourth station, water flows at a slower pace along the path's sides, facilitating optimal sediment deposition for plants.

The flow velocity diminishes to one-third of the speed observed in the main channel along the banks, leading to a corresponding expansion of vegetation. Moving downstream from station 4, an extensive cover extending nearly 2000 m persists, with the most substantial growth occurring in the central region. At station five (see Fig. 5), the combined effects of sedimentation and nutrient absorption have given rise to a dense forest, dominating the highest elevations along the coastal and stream levels. The water velocity at the banks decreases by five to 75 % compared to the speed in the main channel, creating an optimal environment for pollutant absorption. When metals are introduced into the environment, they tend to accumulate in fine particles situated between roots and bed sediments. This accumulation may contribute to the observed increase in vegetation between stations 3 and 4.

This vegetation expansion covers up to 300 m from the shoreline. The final 1000 m of the path, including Station 6, are devoid of vegetation cover. The sixth station has a steeper margin compared to the fourth station. Therefore, the cross-sectional area of the river, which includes the roots and plants, accounts for 3 % of the cross-sectional area of the flow path. This area was 25 % and 12 % at the third and fourth stations, respectively. The water velocity in the middle of the path does not differ from the fourth station, but the flow velocity at the banks is lower than the average velocity in the main channel (Mahsa and Afzalimehr, 2017). The measured values of velocity are 0.06 m/s, at the banks and 0.077 m/s averagely. However, the cross-sectional lateral slope has caused the marsh catchment area at the station to be limited and the width of the vegetation cover to decrease. Fig. 6 shows the graph

Table 4
Hydraulic features, retention time and contact time calculated at each station.

Station	T_{Sc} (min)	T (min)	V_{pa} (m/s)	V_{avg} (m/s)	L_s (m)	T_R (S)	T_R (S)	∀ (m^3)	Q_{pa} (m^3/s)	Q_{avg} (m^3/s)
S1	0	18.52	0	0.09	100	0	0.30	0.006	0	0.02
S2	0	18.3	0	0.1	110	0	7.4	3.85	0	0.52
S3	25	10.53	0.08	0.19	120	10.71	1.14	0.75	0.07	0.66
S4	33.33	25	0.06	0.08	120	48.56	4.37	4.37	0.09	1.00
S5	108.33	54.16	0.02	0.04	130	666.5	9.59	13.33	0.02	1.39
S6	41.66	23.8	0.04	0.07	100	455	11.23	18.2	0.018	1.62

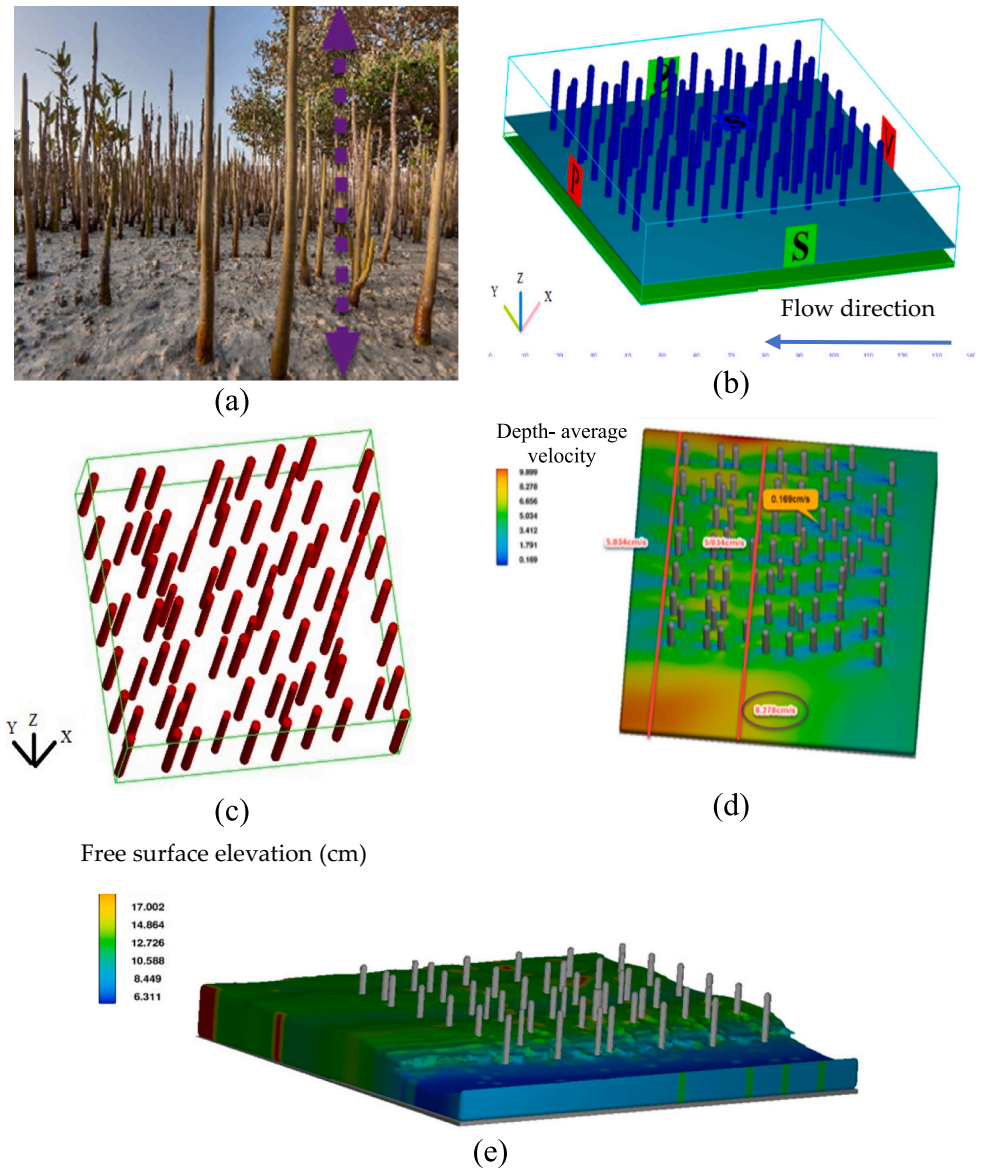

Fig. 4. Hydraulics modeling process a) aerial roots/pneumatophores, b) flow segmentation, c) vegetation cover density d) the simulation of velocity zoning relative to the mean depth and e) changes in water depth.

Fig. 5. Vegetation cover (left) and sediment trap (right) at Station 5.

of density ratio to average velocity.

The impact of the vegetation density on streamflow velocity at six sampling points is depicted in Fig. 6. The figure indicates that vegetation density harms the flow velocity. The lower the density, the higher the velocity. The relatively steep slope of the linear regression line (i.e., correlation coefficient) discovers the immediate impact of the dense

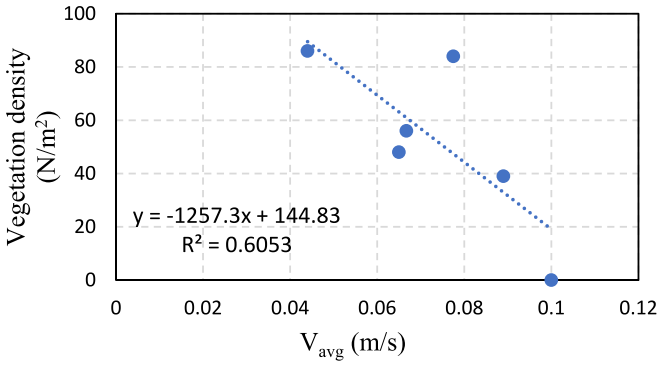

Fig. 6. The graph of plant density over average velocity (effect of root density).

population of mangrove communities on flow velocity. The minimum velocity was recorded at Station 5, which boasts the highest density of vegetation among all stations. The higher the density, the higher the drag coefficient, and according to Morrison's modified formula (Eq. (3)) velocity decreases (Ghanbari, 2015).

$$C_d = \frac{2F_d}{\rho.A.fv^2} \tag{3}$$

Another reason for the velocity reduction could be Newton's law based on the friction between the object (roots) and the fluid (water).

Table 5 represents the results of the laboratory analysis. According to the table, we had the highest absorption at station 4 due to the water flow between the roots. And it is decreasing from station 5. Station 1 has seen high levels of nitrogen and phosphorus, 0.54 and 0.16, due to the stagnant pools caused by the tides. At station 3, due to the growth of plants and the entry of wastewater from the drainage into the main path leading to the wetland, which supplies plant nutrients, the density of plant cover has led to nitrogen absorption and a decrease in phosphorus. Then, at station 4, the trend of pollutant absorption increases. Nitrogen absorption at station 5 is decreasing due to the accumulation mechanism of the rhizosphere and photosynthesis, while phosphorus is increasing. At station 6, due to the proximity to the sea, phosphorus decreased, and nitrogen increased.

A variety of linear and nonlinear regression methods are used to detect underlying patterns in environmental events (Fayaz et al., 2022; Samadi et al., 2020; Zhao et al., 2023). To estimate water quality variables in water systems more accurately, new machine learning models were also suggested (Danandeh Mehr et al., 2023; Shang et al., 2023). According to Fig. 7, nutrient materials are high at the first station and decrease at the second station due to the absence of vegetation, which is the habitat for benthic organisms as nutrients' consumer (Loomer et al., 2023). The nutrient composition increases at the third station with a plant cover density of 56 per square meter due to the biological activity of plants and hard-shelled organisms. At the fourth and fifth station, these values increase in sediment due to the dense vegetation cover of 84.86 N/m^2 and reduced flow, resulting in a significant increase in nutrient compounds. However, at the sixth station, nutrient levels decrease due to the proximity to open waters and their high carbon

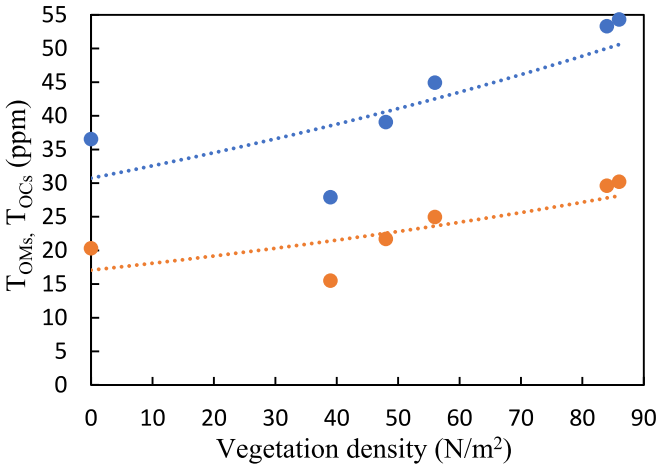

Fig. 7. The change in nutrient chart is indicated by a nonlinear regression for organic maters/carbon and vegetation density in sediment.

content. In general, increased pneumatophore density was found to be positively correlated with higher nutrient levels, including T_{OCs}. Consequently, the stream velocity decreased as it passed through areas with higher pneumatophore density. This resulted in a longer retention time compared to areas with lower density, as illustrated in Fig. 8.

During high tide, the water rises and covers the first station, and the water of the bay fills the sewer canal. During low tide, the water begins to exit, and the water level of the first station quickly decreases, and the water returns from the canal towards the bay. Pollutants, due to the high level of the first station and being far from the main water path, have the lowest level of pollutant in the water and absorption in the sediment according to the results obtained from the measurements performed by the accredited laboratory. At the second station, due to the entry of the industrial town's sewage into the canal, it has a high number of pollutants. After the canal water enters the main flow path at the third station, due to the plant cover and the habitat of crustaceans, very high amounts of nutrients in the water and sediment have been measured (Patrick Jr and DeLaune, 1977). Between the third and fourth stations, the plant cover has decreased, and again from the fourth station due to the high amounts of nutrients, the plants are growing, and at the fifth station, a large volume of mangrove plants have grown, which with the water flow between the roots, the water velocity has come down, and the pollutants are being absorbed and settling. This finding agrees with the results of Nie et al. (2023) in which strong nitrate reduction potential of mangrove ecosystem was highlighted. At the sixth station, the water is becoming stagnant due to the end of the low tide time.

According to Figs. 8 and 9, during the flow, as the plant cover increases, we witness a decrease in velocity between the roots of the pneumatophores, which increases the retention time of the water with the plant and causes the absorption of nutrients, T_{Ns}, and total phosphorus. In fact, the increase in duration has a direct relationship with the absorption of organic matter in the sediment and the removal of organics in the water.

The trend of changes in total nitrogen absorption in sediment and its

Table 5
The results of nutrient concentration in sediment and water from sampling.

Sediment					Water			
Stations	T_{OM} (ppm)	T_{OC} (ppm)	T_N (ppm)	T_P (ppm)	T_{OMw} (ppm)	T_{OCw} (ppm)	T_{Nw} (ppm)	T_{Pw} (ppm)
S1	27.9	15.5	0.54	0.16	0.84	0.87	0.27	2
S2	36.54	20.3	0.14	0.65	0.28	0.156	0.42	2
S3	44.92	24.95	0.64	0.42	1.22	0.331	0.43	2
S4	53.3	29.6	1.42	0.58	0.59	0.682	0.42	2
S5	54.3	30.2	2.1	0.6	0.49	0.273	0.21	2.3
S6	39.06	21.7	2.02	1.48	0.36	0.212	0.31	2

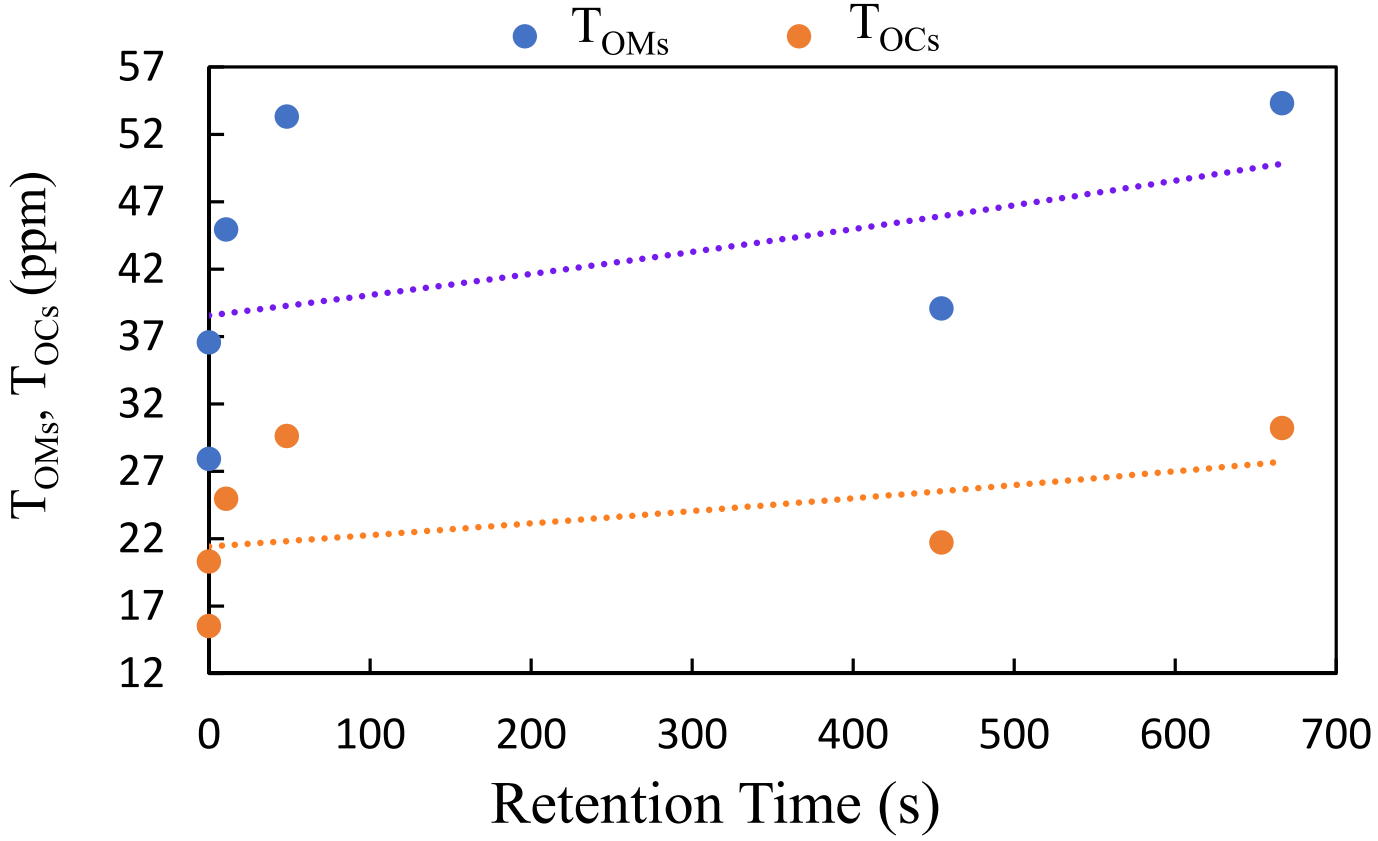

Fig. 8. Changes total organic matter and total organic carbon against retention time in sediment. Dashed lines represent exponential fit.

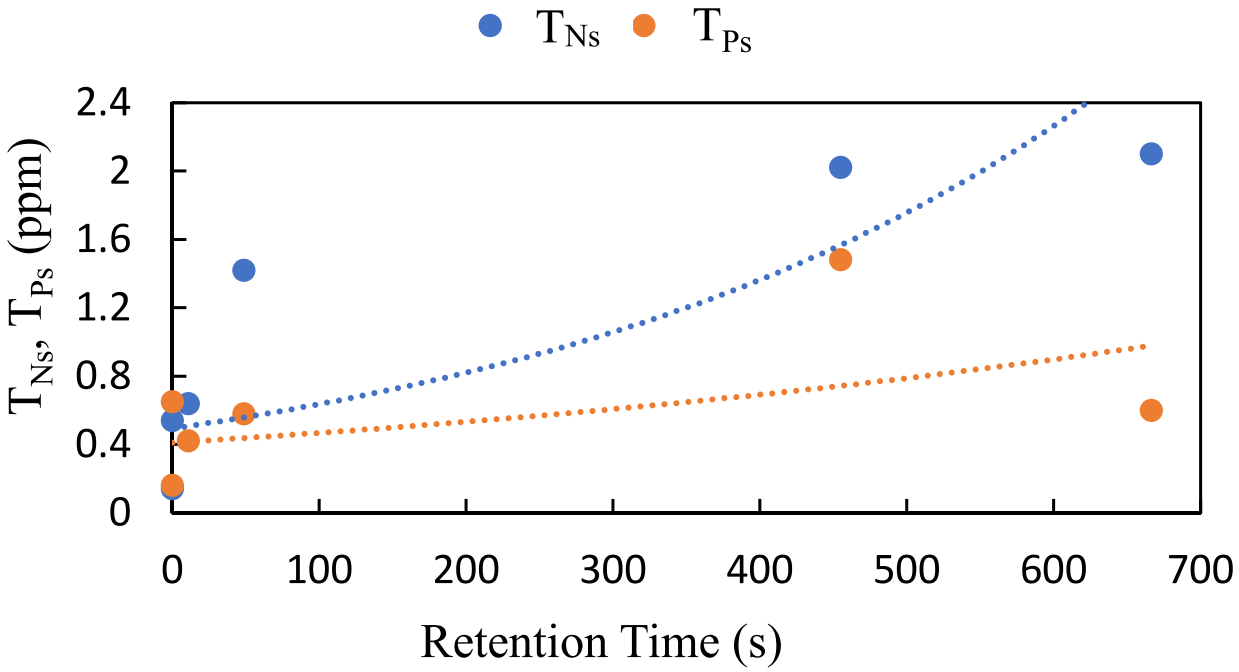

Fig. 9. Change in Total Nitrogen and Total Phosphor against Retention Time in sediment.

removal in water has been ascending and descending respectively. Considering that the longest water retention time between the aerial roots of mangroves according to Fig. 10 is related to the station five, the highest absorption of total nitrogen in the sediment and its removal in the water also happened in this place.

As can be seen, the variation of total nitrogen (T_N) is directly proportional to the retention time coefficient. Upon integrating both sides of Eq. (3), Eq. (4) has been come up. This equation depicts the process of total nitrogen being trapped and absorbed into the sediment (T_{Ns}).

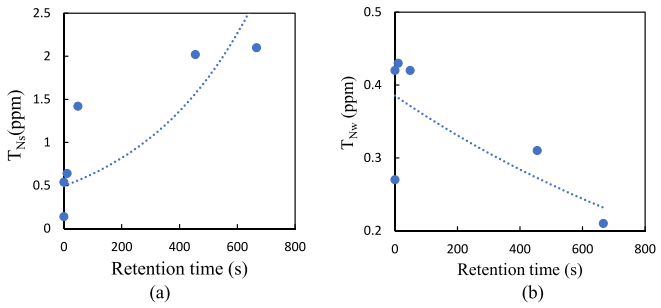

Fig. 10. Total nitrogen changes in (a) sediment and (b) water against retention time.

$$\frac{dT_{Ns}}{dT_R} \approx k.T_R \rightarrow \frac{dT_{Ns}}{dT_R} = k.T_R$$
$$\int dT_{Ns} = \int k.T_R.dT_R \rightarrow T_{Ns} = k\frac{T_R^2}{2} + C; \frac{k}{2} = k' \quad (4)$$

Therefore, in formula (4), T_{Ns} could be described by the following formula.

$$T_{Ns} = k'.T_R^2 + C \quad (5)$$

Eq. 5 is for the second-order reaction model of T_{Ns} variation in salt marsh which is extracted from Fig. 10a as follows:

$$T_{Ns} = \alpha.e^{\beta.T_R} \quad (6)$$

where $\alpha = 0.4942$ and $\beta = 0.0025$ have been demonstrated in Fig. 10a.

In Eq. (7), removal of total nitrogen was observed and described as T_{Nw}. The negative coefficient for retention time in water indicates the removal of total nitrogen from this water versus its absorption by sediment.

$$\frac{dT_{Nw}}{dT_R} \approx -k.T_R \rightarrow \frac{dT_{Nw}}{dT_R} = -k.T_R$$
$$\int dT_{Nw} = \int -k.T_R dT_R \rightarrow T_{Nw} = -k\frac{T_R^2}{2} + C; -\frac{k}{2} = -k \quad (7)$$

where k is constant coefficient for T_{Nw} absorption and T_R is retention time in water for Eq. (7). Eq. (8) is for the First-order reaction model of T_{Nw} variation in water which is obtained from Fig. 10b as follows:

$$T_{Nw} = -k.T_R^2 + C \quad (8)$$

$$T_{Nw} = \alpha.e^{-\beta.T_R} \quad (9)$$

where $\alpha = 0.3855$ and $\beta = -8 \times 10^{-4}$ obtained from Fig. 10b.

To enhance the estimation relationships, we incorporated Eq. (4) into Eq. (9) using the information from Fig. 11. Subsequently, we derived Eq. (10), which yielded results that closely matched the measured values of total nitrogen. Here, T_{Ne} (estimated) represents the derived relationship for total nitrogen absorption in the sediment.

$$T_{Ns} = a.T_{Ne} + b \rightarrow T_{Ne} = k\frac{T_R^2}{2}$$
$$T_{Ns} = a\left(k\frac{T_R^2}{2}\right) + b; \frac{ak}{2} = \xi \quad (10)$$

where $\alpha k/2 = \xi$ is the enhancement constant in the equation of total nitrogen estimation. The values of ξ and b are 0.0029 and 0.7519, respectively.

$$T_{Ns} = \xi\left(T_R^2\right) + b \quad (11)$$

Fig. 12 demonstrates a strong correlation between the duration of retention time and the density of plant cover. The extended retention time is a result of reduced flow between the roots, coupled with their high vegetation density that Eq. (12) extracted from it.

$$T_R = \lambda.den \quad (12)$$

where parameter $\lambda = 3.9153$ is the constant coefficient of vegetation density.

By substituting Eq. (10) into Eq. (5), a new Eq. (13) is obtained which is a function of retention time and vegetation cover density. Additionally, the equation represents a first-order reaction model. As total nitrogen and vegetation both retention time functions, we can combine these functions.

$$T_{Ns} = \alpha.e^{\beta.T_R} \rightarrow T_{Ns} = f(T_R)$$
$$T_R = \lambda.den \rightarrow T_R = g(den)$$
$$T_{Ns} = f(g(den))$$
$$T_{Ns} = \alpha.e^{\beta.T_R} \rightarrow T_{Ns} = \alpha.e^{\beta(\lambda.den)} \quad (13)$$

As β increases, the value of T_{Ns} increases exponentially at a rate determined by the value of T_R. The constant α represents the initial value of the function, or the value of T_{Ns} when β is equal to zero.

In the above equation specifies that α equals 0.4942 and β equals 0.0025. The parameters used in Eqs. (4) to (13), were listed in Table 6.

Our findings reveal parallels in nutrient absorption between sediment and plants, akin to processes observed in wastewater treatment

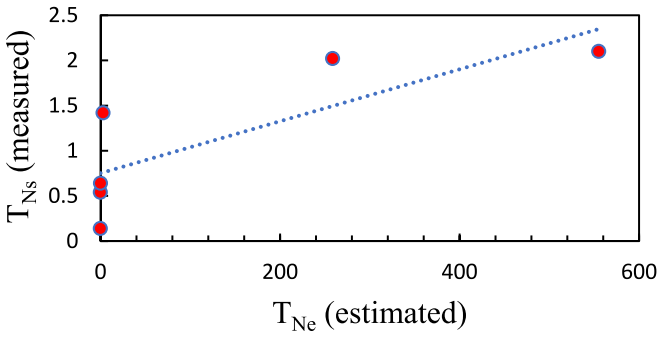

Fig. 11. Measured values T_{Nm} Vs. estimated values of T_{Ne} in sediment.

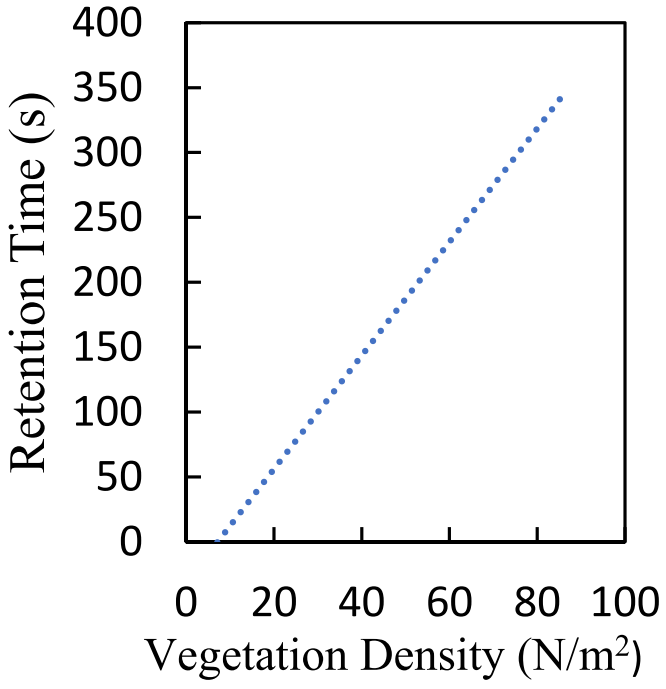

Fig. 12. Changes in retention time against vegetation density.

Table 6
Specifications of the introduced parameters.

Parameter	Symbol	Parameter	Symbol
Retention Time	T_R	Total Nitrogen in Sediment	T_{Ns}
constant coefficient	α	coefficient absorption rate	k'
independent variable	β	Total Nitrogen in water	T_{Nw}
constant coefficient	k	Estimated Total Nitrogen	T_{Ne}
Measured Total Nitrogen	T_{Nm}	enhancement constant	ξ
Vegetation Density	Den	constant coefficient of vegetation density	λ
Total Organic Carbon in sediment	T_{OCs}	Total phosphorus in sediment	T_{Ps}
Total phosphorus in water	T_{Pw}	Total Organic Matter in sediment	T_{OMs}

tanks, where nutrient removal is directly linked to retention time (Krumins et al., 2002). Mangrove species act as ecological indicators, reflecting long-term natural changes when influenced by human activities like sewage disposal, agricultural inputs, and animal manure. They function by absorbing excess nutrients from the ecosystem. Our results align with Tanu et al.'s findings (Tanu et al., 2020), highlighting mangroves' capacity to uptake anthropogenic nitrogen from sediments, promoting vegetation growth. Notably, our research provides initial insights into the impact of river flow on Pneumatophores. Like the studies conducted by (Kumar et al., 2013; Li et al., 2023c), our investigation underscores the sediment surface as the primary adsorbent during the studied period. While acknowledging other factors influencing organic matter and nitrogen in sediment, our study identifies the sedimentation process and flow regime as key contributors to the dynamics of nitrogen and organic matter. These findings align with earlier studies (Hu et al., 2023; Tournoud et al., 2005; Simon and Kennedy, 1987).

Physical effects of Pneumatophores' density (velocity reduction and retention/contact time increase) have the first side-contribution in adsorption of T_N and T_{OM} in coastal wetlands' sediments. However, according to the findings of this research we can add a new headway in the shallow lakes' mechanisms. It would be the sediment adsorption that will come up as the first stage of stream flow velocity decrease in reduction of T_N and T_{OM} concentration in water flow discharging from the terrestrial rivers to the ocean in coastal wetlands area (Xu et al., 2023).

4. Conclusion

The impact of pneumatophores on water flow rate, retention time, contact time, and nutrient absorption through the sediment in subtropical salt marshes was investigated. The results showed how the density of mangroves in salt marshes may influence the kinematic factors of streamflow at estuaries. Regarding Chabahar Bay, we found that the streamflow along the saltmarsh is seriously affected by the tides. Due to the slowing down of velocity and increasing water contact with the plant, water quality variables (such as nitrogen) are absorbed by sediment and pneumatophores. According to the modeling results and field measurements, vegetation density increases flow resistance and causes velocity reduction. As a result, the retention time increases among pneumatophores. On the other hand, the presence of nutrients and organic matter increases the density of vegetation cover (mangrove ecosystem), which in turn reduces flow rate to the sea. This phenomenon can be considered as a threat for the river ecology and human health (i.e., interruption into the ecosystem service) in the future.

Our study also highlighted that the increasing mangrove community acts as a sink for Nitrogen absorption in coastlines. Apart from the above-mentioned consequences, this phenomenon reveals a practical perspective for salt marsh expansion (i.e., reducing pollution load). Thus, the function of salt marsh sediment as a sink makes the coastal wetland as an ecotone natural filter. The results hold significance for the local community, providing a basis to persuade coastal management authorities to allocate financial support for the expansion of coastal vegetation.

CRediT authorship contribution statement

Sadegh Partani: Writing – review & editing, Supervision, Project administration, Methodology, Conceptualization. **Ali Danandeh Mehr:** Writing – review & editing, Investigation, Conceptualization. **Ali Jafari:** Writing – original draft, Software, Formal analysis, Data curation.

Declaration of competing interest

The authors declare the following financial interests/personal relationships which may be considered as potential competing interests: ALI DANANDEH MEHR reports was provided by Antalya Bilim University. If there are other authors, they declare that they have no known competing financial interests or personal relationships that could have appeared to influence the work reported in this paper.

Data availability

Data will be made available on request.

Acknowledgements

We express our gratitude to the two anonymous reviewers for their valuable feedback. The first author acknowledges the Türkiye Scholarships (20IR008182) program, which has afforded him the opportunity to conduct this study partially at Antalya Bilim University.

During the preparation of this work the authors used ChatGPT 3.5 in order to improve language and readability of the revised manuscript. The authors reviewed and edited the content as needed and take full responsibility for the content of the publication.

References

Ahmed, S., Sarker, S.K., Friess, D.A., Kamruzzaman, M., Jacobs, M., Islam, M.A., Pretzsch, H., 2022. Salinity reduces site quality and mangrove forest functions. From monitoring to understanding. Sci. Total Environ. 853, 158662.

Akram, H., Hussain, S., Mazumdar, P., Chua, K.O., Butt, T.E., Harikrishna, J.A., 2023. Mangrove health: a review of functions, threats, and challenges associated with mangrove management practices. Forests 14 (9), 1698. https://doi.org/10.3390/f14091698.

Alongi, D.M., 2018. Impact of global change on nutrient dynamics in mangrove forests. Forests 9 (10), 596.

Baubekova, A., Ahrari, A., Etemadi, H., Klöve, B., Haghighi, A.T., 2024. Environmental flow assessment for intermittent rivers supporting the most poleward mangroves. Sci. Total Environ. 907, 167981.

Behrooz, R.D., Khammar, S., Poma, G., Rajaei, F., 2024 Jan 1. Occurrence and patterns of metals in mangrove forests from the Oman Sea, Iran. Mar. Pollut. Bull. 198, 115866.

Carollo, F.G., Ferro, V., Termini, D., 2005. Flow resistance law in channels with flexible submerged vegetation. J. Hydraul. Eng. 131, 554–564.

Danandeh Mehr, A., Marttila, H., Torabi Haghighi, A.T., Croghan, D., Fathollahzadeh, Attar N., 2023. GTAR: a new ensemble evolutionary autoregressive approach to model dissolved organic carbon. AQUA-water infrastructure. Ecosyst Soc. 72, 381–394.

Ebrahimi, N., Shirdeli, A., Nikkhah Javan, E., Hosseini, M., 2016. The impact of waterways bed's vegetation on flow hydraulic and bed form. Watershed Eng. Manag. 8, 182–192. https://doi.org/10.22092/ijwmse.2019.118083.

EPA US, 1996. USEPA-Method 1669- Sampling Ambient Water for Trace Metals at EPA Water Quality Criteria Level 1996. Water, O, Ed.

Fayaz, S.A., Zaman, M., Butt, M.A., 2022. Numerical and experimental investigation of meteorological data using adaptive linear M5 model tree for the prediction of rainfall. Rev. Comp. Eng. Res. 9 (1), 1–12. https://doi.org/10.18488/76.v9i1.2961.

Ghanbari, Adivi E., 2015. Laboratory study at the impact of coastal green belt on wave attenuation. J. Mar. Sci. Technol. 13, 40–50. https://doi.org/10.22113/jmst.2015.7987.

Hamilton, S.E., Casey, D., 2016. Creation of a high spatio-temporal resolution global database of continuous mangrove forest cover for the 21st century (CGMFC-21). Glob. Ecol. Biogeogr. 25, 729–738.

Hu, S., Cui, K., Chen, Y., Hassan, M., 2023. Comprehensive study of the occurrence and characteristics of organic matter, nitrogen, and phosphorus in sediments and riparian soils of a large drinking water reservoir. Environ. Monit. Assess. 195, 194.

Johnson, J., Morgan, M.F.J., 2010. Plant sampling guidelines. Sampl. Protoc. 1–2.

Kandasamy, K., Rajendran, N., Balakrishnan, B., Thiruganasambandam, R., Narayanasamy, R., 2021. Carbon sequestration and storage in planted mangrove stands of Avicennia marina. Reg. Stud. Mar. Sci. 43, 101701.
Kang, X., Song, J., Yuan, H., Li, X., Li, N., Duan, L., 2017. The sources and composition of organic matter in sediments of the Jiaozhou Bay: implications for environmental changes on a centennial time scale. Acta Oceanol. Sin. 36, 68–78.
Karsch, G., Mukul, S.A., Srivastava, S.K., 2023. Annual mangrove vegetation cover changes (2014–2020) in Indian sundarbans national park using landsat 8 and Google Earth engine. Sustainability 15, 5592.
Krumins, V., Hummerick, M., Levine, L., Strayer, R., Adams, J.L., Bauer, J., 2002 Dec. Effect of hydraulic retention time on inorganic nutrient recovery and biodegradable organics removal in a biofilm reactor treating plant biomass leachate. Bioresour. Technol. 85 (3), 243–248. https://doi.org/10.1016/s0960-8524(02)00129-3 (PMID: 12365490).
Kumar, S.D., Santhanam, P., Jayalakshmi, T., Nandakumar, R., Ananth, S., Devi, A.S., Prasath, B.B., 2013 Jul 1. Optimization of pH and retention time on the removal of nutrients and heavy metal (zinc) using immobilized marine microalga Chlorella marina. Aust. J. Biol. Sci. 13 (5), 400–405.
Lam, K.-L., Lam, Y.-H., Ng, A.Y.-S., So, K.K.-Y., Tam, N.F.-Y., Lee, F.W.-F., Mo, W.-Y., 2023. The impact of anthropogenic pollution on tidal water quality in mangrove wetlands. J. Mar. Sci. Eng. 11, 2374.
Li, R., Zhu, G., Lu, S., Sang, L., Meng, G., Chen, L., Wang, Q., 2023a. Effects of urbanization on the water cycle in the Shiyang River basin: based on a stable isotope method. Hydrol. Earth Syst. Sci. 27 (24), 4437–4452.
Li, W., Wang, W., Sun, R., Li, M., Liu, H., Shi, Y., Fu, S., 2023b. Influence of nitrogen addition on the functional diversity and biomass of fine roots in warm-temperate and subtropical forests. For. Ecol. Manage. 545, 121309.
Li, Z., Li, X., Wang, S., Che, F., Zhang, Y., Yang, P., et al., 2023c. Adsorption and desorption of heavy metals at water sediment interface based on bayesian model. J. Environ. Manage. 329, 117035.
Liu, C., Shen, Y., ming., 2008. Flow structure and sediment transport with impacts of aquatic vegetation. J. Hydrodyn. 20, 461–468.
Liu, J., Wang, Y., Li, Y., Peñuelas, J., Zhao, Y., Sardans, J., Wu, J., 2023. Soil ecological stoichiometry synchronously regulates stream nitrogen and phosphorus concentrations and ratios. CATENA 231, 107357. https://doi.org/10.1016/j.catena.2023.107357.
Loomer, H.A., Kidd, K.A., Erdozain, M., et al., 2023. Stream macroinvertebrate community responses to an agricultural gradient alter consumer-driven nutrient dynamics. Hydrobiologia 850, 315–334. https://doi.org/10.1007/s10750-022-05070-w.
Lovelock, C.E., Feller, I.C., McKee, K.L., Engelbrecht, B.M., Ball, M.C., 2004. The effect of nutrient enrichment on growth, photosynthesis and hydraulic conductance of dwarf mangroves in Panama. Funct. Ecol. 18 (1), 25–33.
Mahsa, Jahadi, Afzalimehr, H., 2017. Flow structure within a vegetation patch in an experimental flume. J. Hydraul. 12, 41–52. https://doi.org/10.30482/jhyd.2017.52007.
Naidu, S.A., Kathiresan, K., Simonson, J.H., Blanchard, A.L., Sanders, C.J., Pérez, A., et al., 2022. Carbon and nitrogen contents driven by organic matter source within Pichavaram wetland sediments. J. Mar. Sci. Eng. 10. https://doi.org/10.3390/jmse10010053.
Nardin, W., Edmonds, D.A., Fagherazzi, S., 2016. Influence of vegetation on spatial patterns of sediment deposition in deltaic islands during flood. Adv. Water Resour. 93, 236–248.
Nellemann, C., Corcoran, E., 2009. Blue Carbon: The Role of Healthy Oceans in Binding Carbon: A Rapid Response Assessment. UNEP/Earthprint.
Nie, S., Mo, S., Gao, T., Yan, B., Shen, P., Kashif, M., Jiang, C., 2023. Coupling effects of nitrate reduction and sulfur oxidation in a subtropical marine mangrove ecosystem with Spartina alterniflora invasion. Sci. Total Environ. 862, 160930.
Numbere, A.O., 2018 Nov 7. Mangrove species distribution and composition, adaptive strategies and ecosystem services in the Niger River Delta, Nigeria. Mangrove Ecosyst. Ecol. Funct. 7, 17.
Olliver, E.A., Edmonds, D.A., Shaw, J.B., 2020. Influence of floods, tides, and vegetation on sediment retention in Wax Lake Delta, Louisiana, USA. J. Geophys. Res. Earth Surf. 125, e2019JF005316.
Partani, S., Mehr, A.D., Maghrebi, M., Mokhtari, R., Nachtnebel, H.P., Taniwaki, R.H., Arzhangi, A., 2023 Dec. A new spatial estimation model and source apportionment of aliphatic hydrocarbons in coastal surface sediments of the Nayband Bay, Persian Gulf. Sci. Total Environ. 15 (904), 166746.
Patrick Jr., W.H., DeLaune, R.D., 1977. Chemical and biological redox systems affecting nutrient availability in the coastal wetlands. Geosci. Man 18, 137.
Pawar, P.R., 2013. Monitoring of impact of anthropogenic inputs on water quality of mangrove ecosystem of Uran, Navi Mumbai, west coast of India. Mar. Pollut. Bull. 75 (1–2), 291–300.
Reef, R., Feller, I.C., Lovelock, C.E., 2010. Nutrition of mangroves. Tree Physiol. 30 (9), 1148–1160.
Rostami, F., Attarod, P., Keshtkar, H., Nazeri, Tahroudi M., 2022. Impact of climatic parameters on the extent of mangrove forests of southern Iran. Casp. J. Environ. Sci. 20, 671–682.
Sadio, C.A.A.S., Faye, C., 2023. Evaluation of extreme flow characteristics in the Casamance watershed upstream of Kolda using the IHA/RVA method. Int. J. Sustain. Energy Environ. Res. 12 (2), 31–45.
Samadi, M., Sarkardeh, H., Jabbari, E., 2020. Explicit data-driven models for prediction of pressure fluctuations occur during turbulent flows on sloping channels. Stoch. Env. Res. Risk A. 34, 691–707. https://doi.org/10.1007/s00477-020-01794-0.
Shang, Y., Song, K., Lai, F., Lyu, L., Liu, G., Fang, C., Wen, Z., 2023. Remote sensing of fluorescent humification levels and its potential environmental linkages in lakes across China. Water Res. 230, 119540 https://doi.org/10.1016/j.watres.2022.119540.
Simmons, K., 2014. Sediment Samples (Operating Procedure No. SESDPROC-200-R3).
Simon, N.S., Kennedy, M.M., 1987. The distribution of nitrogen species and adsorption of ammonium in sediments from the tidal Potomac River and estuary. Estuar. Coast. Shelf Sci. 25, 11–26.
Struve, J., Falconer, R.A., 2001. Hydrodynamic and water quality processes in mangrove regions. J. Coast. Res. 65–75.
Tanu, F.Z., Asakura, Y., Takahashi, S., Hinokidani, K., Nakanishi, Y., 2020 Jan 22. Variation in foliar δ15N reflects anthropogenic nitrogen absorption potential of mangrove forests. Forests 11 (2), 133.
Tournoud, M., Perrin, J., Gimbert, F., Picot, B., 2005. Spatial evolution of nitrogen and phosphorus loads along a small Mediterranean river: implication of bed sediments. Hydrol. Process An. Int. J. 19, 3581–3592.
Van Dijk, W.M., Teske, R., Van de Lageweg, W.I., Kleinhans, M.G., 2013. Effects of vegetation distribution on experimental river channel dynamics. Water Resour. Res. 49, 7558–7574.
van Hespen, R., Hu, Z., Borsje, B., De Dominicis, M., Friess, D.A., Jevrejeva, S., et al., 2023. Mangrove forests as a nature-based solution for coastal flood protection: biophysical and ecological considerations. Water Sci. Eng. 16, 1–13. https://doi.org/10.1016/j.wse.2022.10.004.
Water IWWG on Q of, 1978. Water Quality Surveys: A Guide for the Collection and Interpretation of Water Quality Data. Unesco.
Wen, Z., Shang, Y., Lyu, L., Tao, H., Liu, G., Fang, C., Song, K., 2024. Re-estimating China's lake CO2 flux considering spatiotemporal variability. Environ. Sci. Ecotechnol. 19, 100337 https://doi.org/10.1016/j.ese.2023.100337.
Wimmler, M.C., Bathmann, J., Peters, R., Jiang, J., Walther, M., Lovelock, C.E., Berger, U., 2021. Plant–soil feedbacks in mangrove ecosystems: establishing links between empirical and modelling studies. Trees 35, 1423–1438.
Xu, S., Lu, J., Chen, L., Luo, W., Zhu, S., 2023. Experiment on sediment Ammonia nitrogen release of Chaohu Lake in varying hydrodynamic disturbance. Sustainability 15, 1581.
Yang, W., Zhao, H., Chen, X., Yin, S., Cheng, X., An, S., 2013. Consequences of short-term C4 plant Spartina alterniflora invasions for soil organic carbon dynamics in a coastal wetland of Eastern China. Ecol. Eng. 61, 50–57.
Yasmeen, A., Pumijumnong, N., Arungrat, N., Punwong, P., Sereenonchai, S., Chareonwong, U., 2024 Jan. Nature-based solutions for coastal erosion protection in a changing climate: a cutting-edge analysis of contexts and prospects of the muddy coasts. Estuar. Coast. Shelf Sci. 11, 108632.
Yoshikai, M., Nakamura, T., Suwa, R., Sharma, S., Rollon, R., Yasuoka, J., Nadaoka, K., 2022. Predicting mangrove forest dynamics across a soil salinity gradient using an individual-based vegetation model linked with plant hydraulics. Biogeosciences 19 (6), 1813–1832.
Zahed, M.A., Rouhani, F., Mohajeri, S., Bateni, F., Mohajeri, L., 2010. An overview of Iranian mangrove ecosystems, northern part of the Persian Gulf and Oman Sea. Acta Ecol. Sin. 30, 240–244.
Zhang, T., Song, B., Han, G., Zhao, H., Hu, Q., Zhao, Y., Liu, H., 2023. Effects of coastal wetland reclamation on soil organic carbon, total nitrogen, and total phosphorus in China: a meta-analysis. Land Degrad. Dev. 34 (11), 3340–3349.
Zhao, P., Sanganyado, E., Wang, T., Sun, Z., Jiang, Z., Zeng, M., et al., 2022. Accumulation of nutrients and potentially toxic elements in plants and fishes in restored mangrove ecosystems in South China. Sci. Total Environ. 838, 155964 https://doi.org/10.1016/j.scitotenv.2022.155964.
Zhao, Y., Wang, H., Song, B., Xue, P., Zhang, W., Peth, S., Horn, R., 2023. Characterizing uncertainty in process-based hydraulic modeling, exemplified in a semiarid Inner Mongolia steppe. Geoderma 440, 116713.
Zhu, Y., Dai, H., Yuan, S., 2023. The competition between heterotrophic denitrification and DNRA pathways in hyporheic zone and its impact on the fate of nitrate. J. Hydrol. 626, 130175.